Journal of Alloys and Compounds, 211/212 (1994) 237–240
JALCOM 015

Hydrogen internal friction peak and thermal desorption spectrum in amorphous $Cu_{60}Zr_{40}$

H. Mizubayashi, M. Matsumoto and S. Okuda
Institute of Materials Science, University of Tsukuba, Tsukuba, Ibaraki 305 (Japan)

Abstract

The hydrogen internal friction peak (HIFP) and hydrogen thermal desorption (HTD) in amorphous $Cu_{60}Zr_{40}$ were investigated for hydrogen concentrations $C_H \leqslant 45$ at.%. The C_H dependence of the HIFP suggests the following. The site energy (G) distribution for the Zr_4 sites can be explained as a single gaussian distribution $N_1(G)$. In contrast, the G distribution for the Zr_3Cu_1 sites is composed of two constituents $N_2(G)$ and $N_3(G)$. These features are very similar to those reported in amorphous $Cu_{50}Zr_{50}$ after taking into account the change in chemical composition, suggesting that $N_2(G)$ and $N_3(G)$ correspond to Zr_3Cu_1 sites with different next-nearest-neighbour atoms. The HTD results suggest that in amorphous $Cu_{60}Zr_{40}$ hydrogen-induced structural relaxation proceeds below 650 K for $C_H \leqslant 8$ at.%.

1. Introduction

It is widely accepted that in an early transition metal-later transition metal (ETM–LTM) amorphous alloy A–B hydrogen mostly occupies tetrahedral sites, where the sequence of site energies G is determined by the number of LTM atoms, *i.e.* the B_4, B_3A_1, B_2A_2, B_1A_3 and A_4 sites with increasing G or increasing hydrogen concentration C_H [1–6]. Because of the structural disorder in amorphous alloys (a-alloys), G for each tetrahedron B_hA_{4-h} is expected to vary, reflecting the variation in atomic distances. If this effect can be described by a gaussian distribution [1], $N(G)$ in $a-A_{1-x}B_x$ can be given by

$$N(G)=f_0\sum_{h=0}^{4}\frac{4!}{h!(4-h)!}x^h(1-x)^{4-h}\times\frac{1}{\sigma_h\pi^{1/2}}\exp\left[-\left(\frac{G-G_h}{\sigma_h}\right)^2\right] \qquad (1)$$

where the a-alloy is assumed to be structurally isomorphic and chemically random [5]. f_0 denotes the occupation factor, *i.e.* the number of H atoms per metal atom, reflecting a blocking effect around occupied sites which is assumed here to be constant for any G. G_h and σ_h are the mean value and dispersion of G for the B_hA_{4-h} sites respectively. When the difference between successive G_h values is larger than σ_h, $N(G)$ shows five maxima with increasing G. C_H can be related to $N(G)$ by

$$C_H=\int_0^\infty\frac{N(G)}{1+\exp[(G-\mu)/k_BT]}\,dG\approx\int_0^\mu N(G)\,dG \qquad (2)$$

where k_B denotes the Boltzmann factor and T the temperature. Experimentally, most data for the H content in ETM–LTM a-alloys in the higher C_H range are well explained by eqns. (1) and (2) assuming that H occupies those sites under nearest-neighbour blocking [5, 6], *i.e.* $f_0\approx 1.6$ at $x=0.5$ [6]. For the lower C_H range, studies of the hydrogen internal friction peak (HIFP) in a-$Ni_{35}Ti_{65}$ [7], a-$Cu_{50}Ti_{50}$ [8, 9] and a-$Cu_{50}Zr_{50}$ [10] also support the view of nearest-neighbour blocking. That is, it is suggested that only H atoms occupying sites with site energy $G\approx\mu$ can contribute to hydrogen diffusion in a-alloys, where the total relaxation strength S_t of the HIFP reflects $N(\mu)$ and the profile of the HIFP reflects a distribution of activation energies E, $n(E;\ \mu)$, for reorientation jumps of H atoms between sites with $G\approx\mu$. The HIFP studies on a-$Cu_{50}Zr_{50}$ [10] and a-$Cu_{50}Ti_{50}$ [8, 9] further suggest the following. $N(G)$ for the Zr_4 (or Ti_4) sites can be explained by a single gaussian distribution $N_1(G)$, where the H content attained shows good agreement with the corresponding value expected from eqn. (1). In contrast, $N(G)$ for the Zr_3Cu_1 (Ti_3Cu_1) sites appears to be composed of two constituents $N_2(G)$ and $N_3(G)$, where the total H content in both $N_2(G)$ and $N_3(G)$ shows good agreement with the H content for the Zr_3Cu_1 (Ti_3Cu_1) sites expected from eqn. (1). The distribution $n(E;\ \mu)$ is found to be composed of several constituent gaussian distributions

0925-8388/94/$07.00
SSDI 0925-8388(93)00015-Q

$n_m(E;\ \mu)$ ($m=0$–6 for a-$Cu_{50}Zr_{50}$ or $m=0$–5 for a-$Cu_{50}Ti_{50}$), where differences between neighbouring mean activation energies E_m are larger than the dispersion β_m of E. To clarify whether these characteristic features found for the HIFP reflect a common property of ETM–LTM a-alloys, we further investigated the C_H dependence of the HIFP in a-$Cu_{60}Zr_{40}$ here. Separately we also investigated the hydrogen thermal desorption (HTD) [9–12] from a-$Cu_{60}Zr_{40}$ in ref. 13 to gain insight into $N(G)$ on the G scale, which will be discussed together with the HIFP results.

2. Experimental procedures

Amorphous $Cu_{60}Zr_{40}$ was prepared by melt spinning in a high purity Ar gas atmosphere. Hydrogen charging was done electrolytically and then the specimens were mechanically polished in water to remove the surface layer. The size of the specimens was about 10 μm × 1 mm × 10 mm. The hydrogenated specimens were aged for a few days at room temperature (RT) to homogenize C_H in them and then subjected to HIFP measurements. After the HIFP measurements the specimens were subjected to vacuum extraction to determine C_H [13]. The HIFP was measured using the resonant flexural vibration of about 500 Hz of specimens with a strain amplitude of 10^{-6}, where the resonant frequency $f \propto M^{1/2}$ and the internal friction Q^{-1} were almost continuously measured against temperature T, where M is the Young modulus of the specimens (see refs. 8–10 for the detailed measuring procedures).

3. Results and discussion

Figure 1 shows examples of the HIFP observed in a-$Cu_{60}Zr_{40}$ specimens with various $C_H \leqslant 32$ at.% (100[H]/[metal]). The HIFP is observed as a very broad peak over the entire T range below 350 K, exhibiting a maximum between about 200 and 320 K. Q^{-1} in the a-$Cu_{60}Zr_{40}$ specimen without hydrogen charging is very low, except for a trace of the HIFP at RT due to H which was possibly absorbed into the specimen during polishing. After H charging, the HIFP maximum grows at around 320 K at first, then shows a repetition of decrease and increase as well as a general tendency of decreasing T at the HIFP maximum (T_{HIFP}) with increasing C_H. The general features of both the HIFP and the C_H dependence of the HIFP found in a-$Cu_{60}Zr_{40}$ are very similar to those reported in a-$Cu_{50}Zr_{50}$ [10] and a-$Cu_{50}Ti_{50}$ [9], including the features for $n(E;\ \mu)$ (not shown here), when they are compared on the $N(G)$ scale given in eqn. (1), except for the following. In a-$Cu_{60}Zr_{40}$, with increasing C_H, $\Delta T/T_{HIFP}$ decreases from about 0.41 at the middle of $N_1(G)$ to about 0.40 at the middle of $N_2(G)$, and T_{HIFP} at the middle of $N_1(G)$ decreases by about 16% at the middle of $N_2(G)$, where $\Delta T/T_{HIFP}$ is the width of the HIFP at half-maximum normalized by T_{HIFP} (see Fig. 3 for $N_1(G)$ and $N_2(G)$). The corresponding C_H dependence reported is a decrease in $\Delta T/T_{HIFP}$ from about 0.42 to about 0.38 and a decrease in T_{HIFP} by about 10% in a-$Cu_{50}Zr_{50}$, and a decrease in $\Delta T/T_{HIFP}$ from about 0.60 to about 0.33 and a decrease in T_{HIFP} by about 8% in a-$Cu_{50}Ti_{50}$. That is, the features for $\Delta T/T_{HIFP}$ found in a-$Cu_{60}Zr_{40}$ are similar to those reported in a-$Cu_{50}Zr_{50}$ but different from those reported in a-$Cu_{50}Ti_{50}$, and the change in T_{HIFP} with increasing C_H is much larger in a-$Cu_{60}Zr_{40}$ than in a-$Cu_{50}Zr_{50}$ or a-$Cu_{50}Ti_{50}$. These results will be discussed later on.

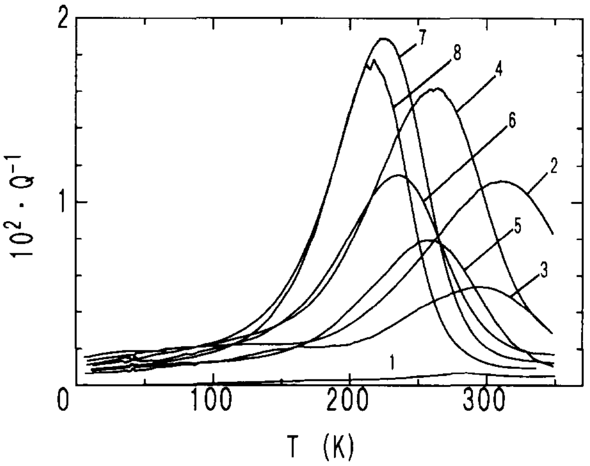

Fig. 1. Hydrogen internal friction peak observed at about 500 Hz in a-$Cu_{60}Zr_{40}$ specimens with various hydrogen concentrations C_H (at.%): 1, ≈0; 2, 3.9; 3, 6.0; 4, 8.7; 5, 10.3; 6, 15.9; 7, 22.2; 8, 31.6.

In Fig. 2 the change in M between 5 and 350 K, $|\Delta M_{350\,K}/M|$, deduced from the observed change in f is plotted against S_t estimated from the observed HIFP (see refs. 9 and 10 for the estimation of S_t). The ordinary temperature change $|\Delta M_T/M|$ is found to be 0.07, which is almost the same as that reported in a-$Cu_{50}Zr_{50}$ or a-$Cu_{50}Ti_{50}$. We estimated the strength of the relaxation of the modulus associated with the HIFP, $|\Delta M_R/M|$, from $|\Delta M_{350\,K}/M|$ after the subtraction of $|\Delta M_T/M|$. As seen in Fig. 2, the relationship $|\Delta M_R/M| = S_t$ can be seen as well as in a-$Cu_{50}Zr_{50}$ [10] and a-$Cu_{50}Ti_{50}$ [9], suggesting that the HIFP in these a-alloys can be well explained by a Debye relaxation process.

Figure 3 shows the C_H dependence of S_t observed in a-$Cu_{60}Zr_{40}$, where curves 1–4 are fitted to the data assuming that all the constituent distributions $N_1(G)$ to $N_4(G)$ are explained by a gaussian distribution. For C_H below about 2 at.% the HIFP is very low. We surmise that some Zr clusters existing even in the amorphous state as reported in a-$Cu_{24}Zr_{76}$ [5] are

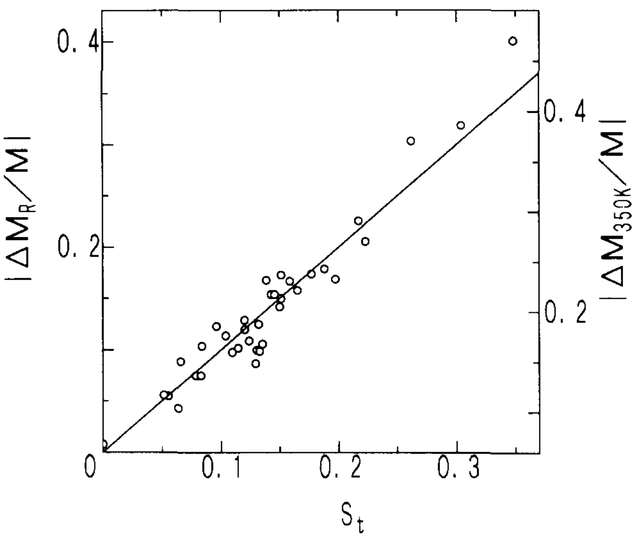

Fig. 2. Modulus change $|\Delta M_{350\,K}/M|$ and that associated with HIFP, $|\Delta M_R/M|$, plotted *vs.* total relaxation strength S_t for HIFP observed in a-$Cu_{60}Zr_{40}$. The straight line is fitted to the data assuming the relationship $|\Delta M_R/M| = S_t$.

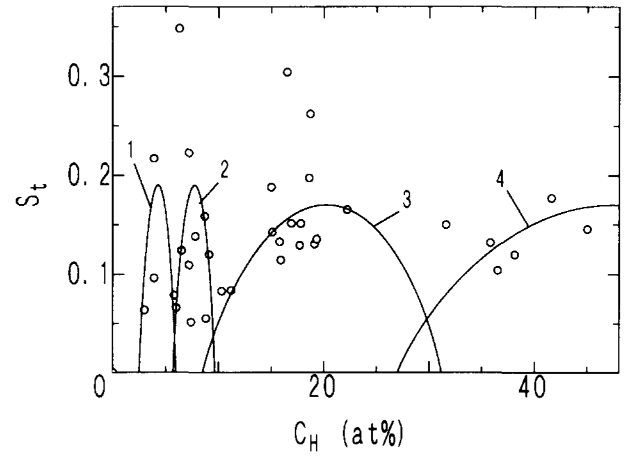

Fig. 3. S_t *vs.* C_H observed for HIFP in a-$Cu_{60}Zr_{40}$. See text for explanation of curves 1–4.

responsible for the very low HIFP below about 2 at.%. For C_H above about 2 at.%, besides the general C_H dependence of S_t estimated as curves 1–4, some scatter in the S_t data can be seen at C_H values of about 7 and 17 at.%, which will be mentioned later. As seen in Fig. 3, the H content attained in $N_1(G)$ is about 4 at.% and that in $N_2(G)+N_3(G)$ about 24 at.%. These show reasonable agreement with the H content of about 4 at.% in the Zr_4 sites and that of about 25 at.% in the Zr_3Cu_1 sites respectively expected from eqn. (1) assuming $f_0 \approx 1.6$ [6]. That is, similar features to those for $N_1(G)$ *and* $N_2(G)+N_3(G)$ reported in a-$Cu_{50}Zr_{50}$ [10] are again observed in a-$Cu_{60}Zr_{40}$. In a-$Cu_{50}Zr_{50}$ [10], $N_2(G)$ and $N_3(G)$ are surmised to correspond to Zr_3Cu_1 sites with different next-nearest-neighbour metal atoms. If that is the case, the relative H content for $N_3(G)/[N_2(G)+N_3(G)]$ is expected to be increased in a-$Cu_{60}Zr_{40}$ owing to an increased Cu content in the a-alloy. In fact, the $N_3(G)/[N_2(G)+N_3(G)]$ value of about 22 at.%/37 at.% ≈ 0.6 reported in a-$Cu_{50}Zr_{50}$ increases to about 20 at.%/24 at.% ≈ 0.8 in a-$Cu_{60}Zr_{40}$ here.

Figure 4 shows examples of HTD spectra observed in a-$Cu_{60}Zr_{40}$ specimens at a heating rate of 1.6 K s^{-1}, which are a redrawing of Fig. 4 reported in ref. 13. The vertical dashed line denotes the crystallization temperature T_x found for a-$Cu_{60}Zr_{40}$ specimens at a heating rate of 1.6 K s^{-1}. As seen in Fig. 4, HTD below T_x is very low for $C_H \leqslant 8$ at.%. For $C_H \geqslant 8$ at.% an HTD peak at around 750 K grows at first, then shows a strong decrease at about 18 at.%. For $C_H \geqslant 18$ at.% an HTD peak is again observed at around 750 K but with a different feature. The growth followed by a decrease in the HTD peak below T_x is also observed for a small HTD peak at around 660 K between about 28 and 34 at.% as well as for a broad HTD peak at around 600 K between about 38 and 48 at.%. The decrease after the growth of the HTD peaks is found to be due to partial crystallization during heating, *i.e.* its onset temperature $T_{x,s}$ decreases with increasing C_H in a-$Cu_{60}Zr_{40}$ [13] (see also ref. 14). Apart from $T_{x,s}$, we observed that HTD below T_x is very low for $C_H \leqslant 8$ at.%, where an HTD peak from the Zr_4 sites can be expected at around 650 K as reported for a-$Cu_{50}Zr_{50}$

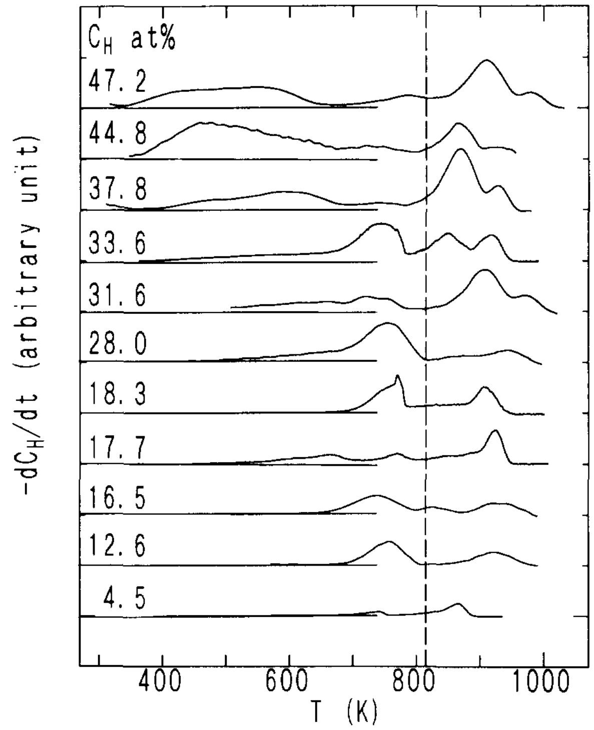

Fig. 4. Hydrogen thermal desorption spectra observed at a heating rate of 1.6 K s^{-1} for a-$Cu_{60}Zr_{40}$ specimens with various hydrogen concentrations C_H as indicated. The vertical dashed line denotes the crystallization temperature for the a-$Cu_{60}Zr_{40}$ specimen without hydrogen charging; here $T_x \approx 815$ K at a heating rate of 1.6 K s^{-1}.

[13]. This fact suggests that H-induced structural relaxation (HISR) proceeds below 650 K in a-$Cu_{60}Zr_{40}$ for $C_H \leqslant 8$ at.%. In a-$Cu_{50}Zr_{50}$ the following is reported [13]. $T_{x,s}$ hardly shows a deviation from T_x for this a-alloy for $C_H \leqslant 40$ at.%, but HISR proceeds intermittently on the C_H scale, showing a decrease in the onset temperature for HISR with increasing C_H down to RT at $C_H \approx 25$ at.%. Correspondingly, the S_t *vs.* C_H data for the HIFP in a-$Cu_{50}Zr_{50}$ show some deviatory scattering from the proper C_H dependence of S_t [10]. Therefore we tentatively surmise that the deviatory scattering from the proper C_H dependence of S_t observed in a-$Cu_{60}Zr_{40}$ (see Fig. 3) presumably reflects the effect of HISR. However, the fact that for both a-$Cu_{60}Zr_{40}$ and a-$Cu_{50}Zr_{50}$ the hydrogen content for $N_1(G)$ and $N_2(G)+N_3(G)$ can be well explained by eqn. (1) suggests that the densities of sites for $N_1(G)$ and $N_2(G)+N_3(G)$ remain unchanged after HISR.

The results for $\Delta T/T_{HIFP}$ mentioned in connection with Fig. 1 suggest that for both a-$Cu_{60}Zr_{40}$ and a-$Cu_{50}Zr_{50}$ the variations in atomic distances in Zr_4 tetrahedra are similar to those in Zr_3Cu_1 tetrahedra, but for a-$Cu_{50}Ti_{50}$ those in Ti_4 tetrahedra are much larger than those in Ti_3Cu_1 tetrahedra. On the other hand, because the relative change in T_{HIFP} between the HIFP for the $Zr_4(Ti_4)$ sites and the HIFP for the $Zr_3Cu_1(Ti_3Cu_1)$ sites is much larger in a-$Cu_{60}Zr_{40}$ than in a-$Cu_{50}Zr_{50}$ or a-$Cu_{50}Ti_{50}$, we surmise that it reflects a change in the number of Cu atoms as next-nearest-neighbour atoms around these sites. To clarify these issues, however, further work is needed.

4. Conclusions

The hydrogen internal friction peak and hydrogen thermal desorption in a-$Cu_{60}Zr_{40}$ were investigated. The C_H dependence of the HIFP suggests the following. The site energy (G) distribution for the Zr_4 sites can be explained as a single gaussian distribution $N_1(G)$, while that for the Zr_3Cu_1 sites is composed of two constituents $N_2(G)$ and $N_3(G)$. These features are very similar to those reported in a-$Cu_{50}Zr_{50}$, suggesting that $N_2(G)$ and $N_3(G)$ correspond to Zr_3Cu_1 sites with different next-nearest-neighbour atoms. The HTD results suggest that in a-$Cu_{60}Zr_{40}$, hydrogen-induced structural relaxation proceeds below 650 K for $C_H \leqslant 8$ at.%.

Acknowledgments

The authors would like to thank Dr. H. Tanimoto for his invaluable help in the course of the experiments. This work is partly supported by a Grant in Aid for Scientific Research from the Ministry of Education, Science and Culture of Japan.

References

1 R. Kirchheim, F. Sommer and G. Schluckbier, *Acta Metall., 30* (1982) 1059.
2 K. Suzuki, *J. Less-Common Met., 89* (1983) 183.
3 K. Kai, S. Ikeda, T. Fukunaga, N. Watanabe and K. Suzuki, *Physica B, 120* (1983) 342.
4 A. Sadoc and J.L. Lasjaunias, *J. Phys. F: Met. Phys., 15* (1985) 1021.
5 J.H. Harris, W.A. Curtin and M.A. Tenhover, *Phys. Rev. B, 36* (1987) 5784.
6 R. Kirchheim, W. Kieninger, X.Y. Huang, S.M. Filipek, J. Rush and T. Udovic, *J. Less-Common Met., 172–174* (1991) 880.
7 U. Stolz, M. Weller and R. Kirchheim, *Scr. Metall., 20* (1986) 1361.
8 H. Mizubayashi, Y. Katoh and S. Okuda, *Phys. Status Solidi A, 104* (1987) 469.
9 H. Mizubayashi, H. Agari and S. Okuda, *Phys. Status Solidi A, 122* (1990) 221.
10 H. Mizubayashi, T. Naruse and S. Okuda, *Phys. Status Solidi A, 132* (1992) 79.
11 T. Araki, T. Abe and K. Tanaka, *Trans. Jpn. Inst. Met., 30* (1989) 748.
12 K. Tanaka, T. Arai, T. Abe and O. Yoshinari, *J. Less-Common Met., 172–174* (1991) 928.
13 H. Mizubayashi, M. Matsumoto, H. Itoh and S. Okuda, *Mater. Sci. Eng. A,* in press.
14 K. Dini and R.A. Dunlap, *J. Phys. F: Met. Phys., 15* (1985) 273.